

Transient models for curve squeal noise

J.F. Brunel^{a,*}, P. Dufrénoy^a, M. Naït^a, J.L. Muñoz^a, F. Demilly^b

^aLaboratoire de Mécanique de Lille CNRS UMR 8107, Cité Scientifique, 59655 Villeneuve d'Ascq, France

^bValdunes, B.P. 129, 59943 Dunkerque, France

Accepted 26 August 2005

Available online 13 February 2006

Abstract

The paper deals with numerical models of railway wheel noise occurring in narrow curves. Curve squeal is presumed to issue from a lateral creepage of the wheels on the rail head. The frequency range is from around 400 to almost 8000 Hz, with noise levels up to 120 dB close to the wheel. Lateral friction forces are induced on the wheel–rail contact area (typically stick-slip forces). Due to nonlinearities of friction forces, a transient analysis of the lateral creepage of the wheel is performed by using an axi-harmonic model. Results give a reduced number of excited modes. It is shown that squealing modes have 3, 4 and 5 nodal diameters. These results agree with experimental investigations of squeal noise measurements. An extension of the transient model is finally discussed. It consists to study the efficiency of a noise attenuation system made of a metallic ring inserted into grooves machined into the wheel.

© 2006 Elsevier Ltd. All rights reserved.

1. Introduction

Squeal noise remains complex to study because of the many physical interactions of the mechanical, tribological and acoustical behaviours. The frequency range extends from 400 to 8000 Hz. According to Rudd [1], excitation mechanisms are related to stick-slip phenomena in the lateral direction on the wheel/rail interface. A great number of wheel modes are excited leading to acoustic emission with overall pressure level up to 120 dB close the wheel [2].

At the macroscopic scale, friction forces are dependant on various parameters: the friction–velocity behaviour, the curve radius of the track, the modal behaviour of the wheel, the wheel loading and the material surface properties [3,4]. A lateral friction force model is discussed in the following. In order to consider the friction phenomena at the contact area, a transient analysis of the lateral creepage of the wheel is performed with an axi-harmonic finite element model. Boundary conditions, lateral and normal forces are decomposed in Fourier series around the circumference. Friction characteristics are implemented in an external contact algorithm.

Finally, an extension of the transient model is discussed. It is used to study the efficiency of a noise attenuation system made of a metallic ring inserted into grooves machined into the wheel. A three-dimensional contact algorithm is introduced in order to highlight attenuation mechanisms.

*Corresponding author. Tel.: +33 3 20 43 65 14; fax: +33 3 28 76 73 01.

E-mail address: jean-francois.brunel@polytech-lille.fr (J.F. Brunel).

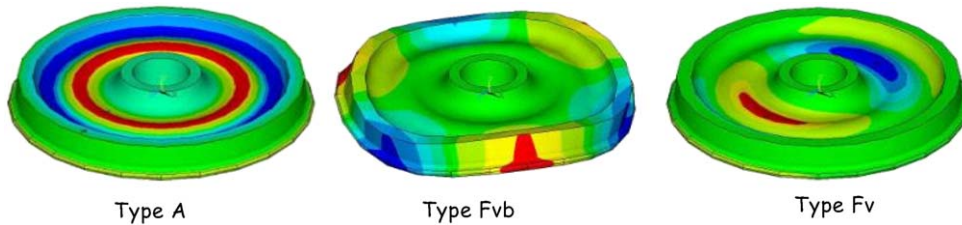


Fig. 1. Modal shapes of the wheel.

2. Background

2.1. Model of the wheel

Three-dimensional and axisymmetric finite element models of the wheel have been developed to determine wheel modes. They are compared with experimental measurements [5]. Three types of modal shapes may be distinguished (Fig. 1):

- Axial modes: $A m$
- Bending of the tread and the web: $Fvb n-m$
- Bending of the web: $Fv n-m$

n and m are, respectively, the number of nodal diameters and the number of nodal circles.

Note that the first mode type refers to in-plane (radial) modes and the two last refer to out-of-plane (axial or bending) modes, according to Ref. [2].

2.2. Harmonic model and tool for radiation computation

A first model has been developed to determine the forced response of an axially excited wheel with a static force in the radial direction representing the vertical load applied on the wheel [6]. Since the problem is linear, a classical superposition method is used to determine the wheel response in the range 0–4000 Hz. The acoustic power radiated is calculated by FEM or BEM. Numerical results show a great number of peaks in the power spectrum with sound power level greater than 100 dB. The identified modes are simply resonant in the sense of the forced response of the linear system submitted to a wide band excitation. Note that the experimental squealing mode appears in the spectrum.

2.3. Squeal mechanisms

The angle of attack, obtained from the curving dynamics, induces friction forces leading to unstable wheel behaviour as curve squeal. Experimental investigations show a relation between squeal occurrence and friction–velocity weakening [7]. Others parameters apart from the friction–velocity relation act on the squeal occurrence [4]: the curve radius of the track, the wheel loading conditions and the modal behaviour of the wheel (damping, mass, stiffness).

All published squeal models are based on the same mechanism, first proposed by Rudd [1]: the wheel slides laterally on the rail head. Squeal models proposed in the literature are developed at the macroscopic scale, without contact patch discretization [8,9]. Instabilities are introduced by the friction–velocity weakening. In this paper, we focus on the friction–velocity relation.

3. Transient axi-harmonic model

3.1. Excitation model

In order to consider the friction–velocity behaviour, the model is improved by an axial component force depending on the slip velocity. The curvature radii of the rail, the contact point position on the wheel rim and

the contact area have not been taken into account in this model. Boundary conditions are described as follows (Fig. 2 on the left):

Displacement of the hub: according to $z = Vt$, V is the lateral speed of the train during the passage of the curve; it is assumed to be constant. The displacements of the wheel hub are constrained to simulate the sliding velocity due to the yaw angle.

Wheel/rail contact forces: the excitation is assumed to have two components:

- a normal load F_n (radial),
- a tangential force (axial) obtained from the friction–velocity relation $F_t = f(V_g^C)$, V_g^C is the slip velocity at the contact point C .

As discussed previously, two types of friction–velocity relation are considered for the condition of squeal occurrence (Fig. 2 on the right). These friction laws are identified from experimental measurements performed by Kooijman et al. [7].

The friction law is given by the relation: $\mu = \mu_d(2/\pi)\arctan(V_g^C/C)$, with C the relative sliding velocity. The negative friction–velocity slope is approximated with: $\mu = (2/\pi)\arctan(V_g^C/C)(\mu_d + (\mu_s - \mu_d)e^{-|\alpha V_g^C|})$, μ_s and μ_d are, respectively, the static and the dynamic friction coefficients and α a decay parameter. Values used in the simulations are summarized in Table 1.

3.2. Mathematical model

A two-dimensional axi-symmetric model is used to reduce the computation time compared with a three-dimensional model. The third dimension (circumferential coordinate θ) is added using a Fourier transformation to introduce non axi-symmetric contact forces. Excitation and displacements are defined as a series of harmonic functions (Fourier series). The origin of the circumferential coordinate θ is chosen so that only cosine terms are calculated in the Fourier series. Displacements fields are:

$$u_r = \sum_n u_{rn} \cos n\theta, \quad u_z = \sum_n u_{zn} \cos n\theta, \quad u_\theta = \sum_n u_{\theta n} \sin n\theta. \tag{1}$$

The convergence speed is dependant on the loading Fourier series. As the excitation is assumed to be a concentrated load, it is necessary to consider up to $n = 7$ harmonic waves, the others can be neglected. The loading is

$$P = \frac{P}{\pi} + \sum_{n=1}^{\infty} \frac{P}{2\pi} \cos n\theta. \tag{2}$$

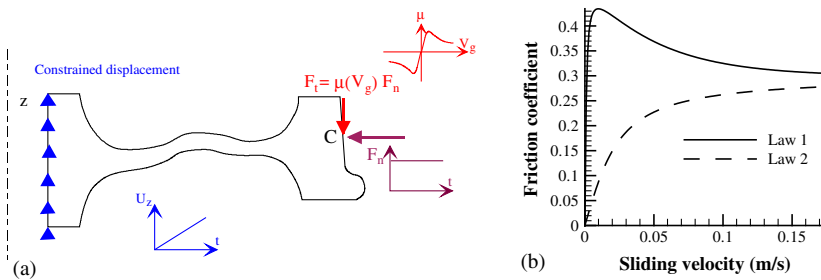


Fig. 2. Axi-harmonic model and friction–velocity relation.

Table 1
Parameters used in the simulation

$F_n = -50,000$ N	$\alpha = 20$
$\mu_d = 0.5$	$C = 1000$ m/s
$\mu_s = 0.3$	$V = 0.05$ m/s

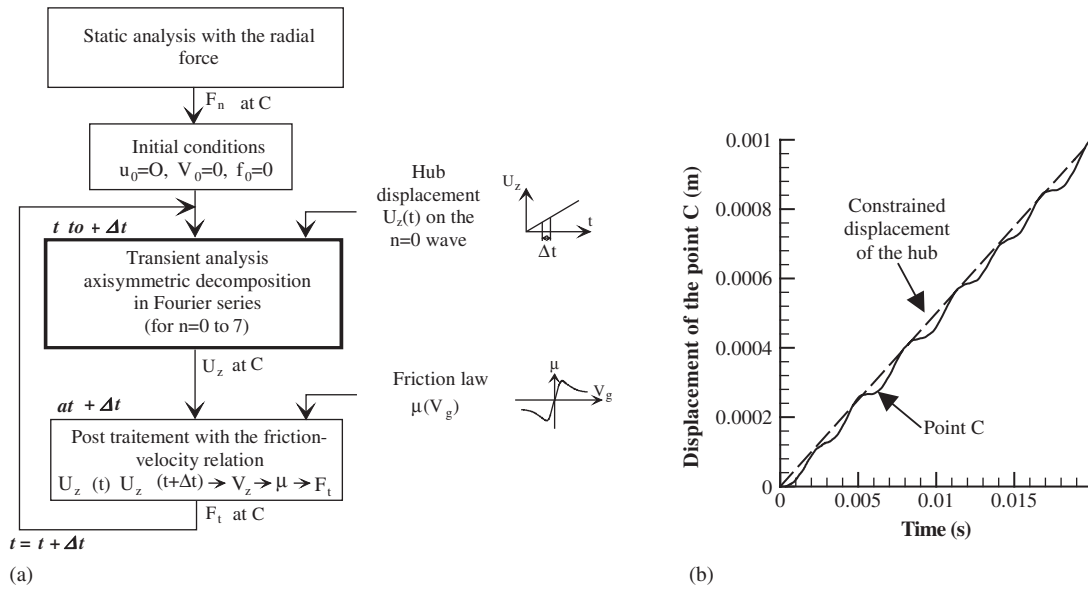


Fig. 3. Transient analysis with the friction–velocity relation.

The 8 computations are solved at the same time. The imposed displacements of the hub are only constrained in the $n = 0$ harmonic wave (axisymmetric term) (Fig. 3a). As the wheel–rail contact is nonlinear, it is solved separately. The transient analysis is solved using an external algorithm presented in Fig. 3 on the left.

3.3. Results

Due to the decomposition, displacement fields are obtained by summation of the Fourier series from 0 to 7. Fig. 3b shows the contact point displacement compared with the hub boundary condition. Variations correspond to lateral oscillations on the wheel–rail contact point (stick-slip phenomenon). For these simulations, the solution converges to a limit cycle, even if the friction law is positive. This is due to the coupling of the normal and lateral dynamics by the Poisson ratio of the wheel material (sprag-slip phenomena).

A Fourier transformation is used to determine wheel displacement spectrum for each harmonic wave. Vibratory spectra are calculated between 0.01 and 0.02 s according to the wheel damping ratio. For $n = 0, 1, 2, 6, 7$, vibratory spectra between the two cases are similar with lower amplitudes. For $n = 3, 4, 5$ velocity peaks on wheel modes are obtained with the two friction laws (Fig. 4). However, levels are greater with the first law.

Squealing modes may be identified as Fvb 3-0, Fvb 4-0 and Fvb 5-0 modes. Note that these mode values may vary slightly with the considered friction law. However, identified modes correspond to experimental values: 1100 and 2000 Hz for, respectively, the Fvb 3-0 and Fvb 4-0 modes [10].

4. Squeal noise attenuation by the ring damping solution

4.1. Presentation and efficiency of the solution

A simple way of increasing the wheel damping is to machine semi-cylindrical grooves into the wheel rim and to insert a circular ring into these grooves (Fig. 5). The ring is open when it is inserted into the groove and secondly welded on its extremities. One or two rings can be used. Acoustic measurements have been performed for application in Hong-Kong application; a sound level attenuation of 10 dB is obtained between existing wheels and ring damped wheels at a distance of about 2 m from the track [11] (Fig. 6). Nevertheless, the same

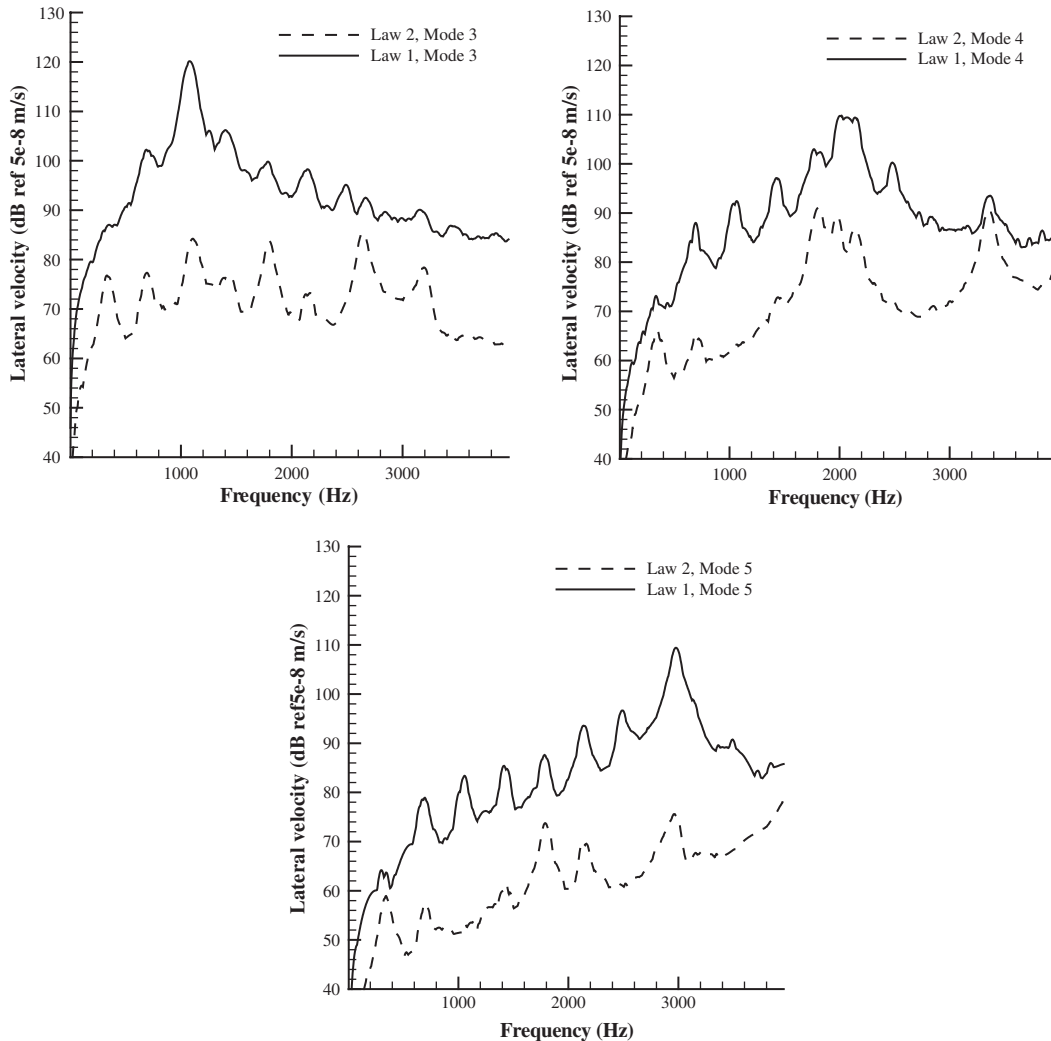


Fig. 4. Wheel displacement spectra for different harmonic waves $n = 3-5$.

ring damped solution has been inefficient for other applications with no obvious explanation. Understanding of the physical mechanisms and ways of optimization of such damping system still remain to be found.

Parameters which act on the efficiency of the solution are the number of rings, their position, their mass and the assembly into the groove. There is no control of contact uniformity and tightness around the circumference. Other solutions have been proposed to control the contact pressure between the ring and the wheel rim [12,13]. For the ring damping solution, experimental investigations have shown that efficiency of the ring damping solution also strongly depends on the assembly conditions [14].

4.2. Origin of the attenuation

In order to highlight the origin of the attenuation, a preliminary axisymmetric model has been developed [6]. Contact of the ring into the groove seems to dissipate enough energy to reduce the web amplitudes. Due to nonlinearity of contact, a transient analysis has been performed; the acoustic intensity is evaluated with a progressive plane wave assumption.

Results show that preload of the ring into the groove is a major factor for frictional contact dissipation and acoustic attenuation (Fig. 7). Even for the optimal value of preload calculation, results give low acoustic

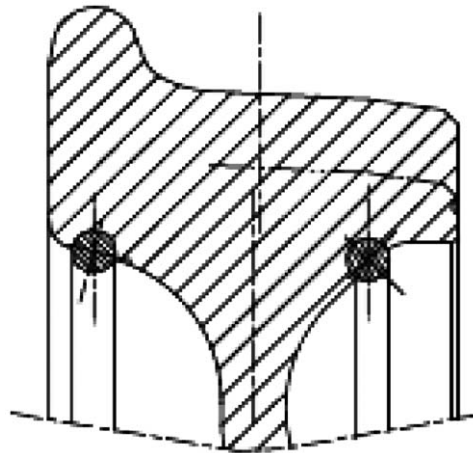


Fig. 5. Ring damping solution.

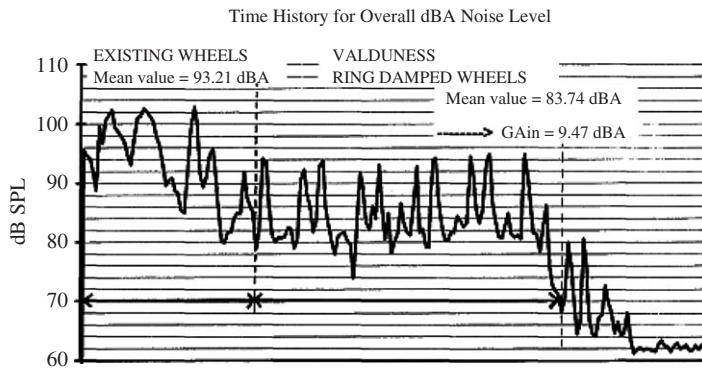


Fig. 6. Time history noise level for undamped and ring damped wheel.

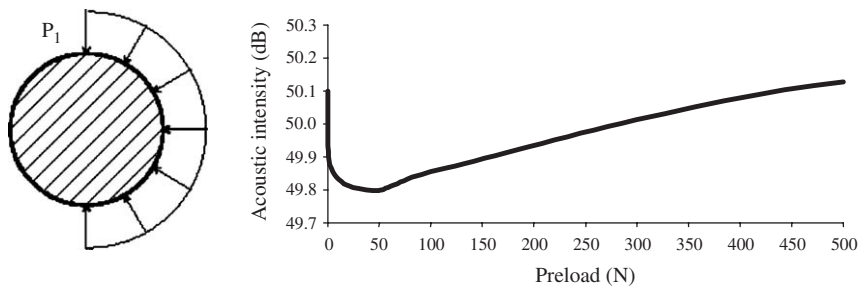


Fig. 7. Influence of preload on acoustic intensity.

attenuation less than 1 dB, compared to 10 dB measured in normal use. Several ways of explanation may be distinguished: the axisymmetric loading assumption, the simplified acoustic model and the preload model.

In order to obtain more reliable quantitative results, a more realistic three-dimensional model has been developed with surface contact elements (Fig. 8a). A transient analysis is performed because of the nonlinearity of contact, with a Lagrangian contact algorithm. Friction coefficient is assumed to be constant ($\mu = 0.3$). The excitation is simplified as a radial static force and an axial harmonic force so that the Fvb 3-0 mode is investigated (identified as a squeal mode, 1106 Hz). No friction characteristic has been implemented in this model.

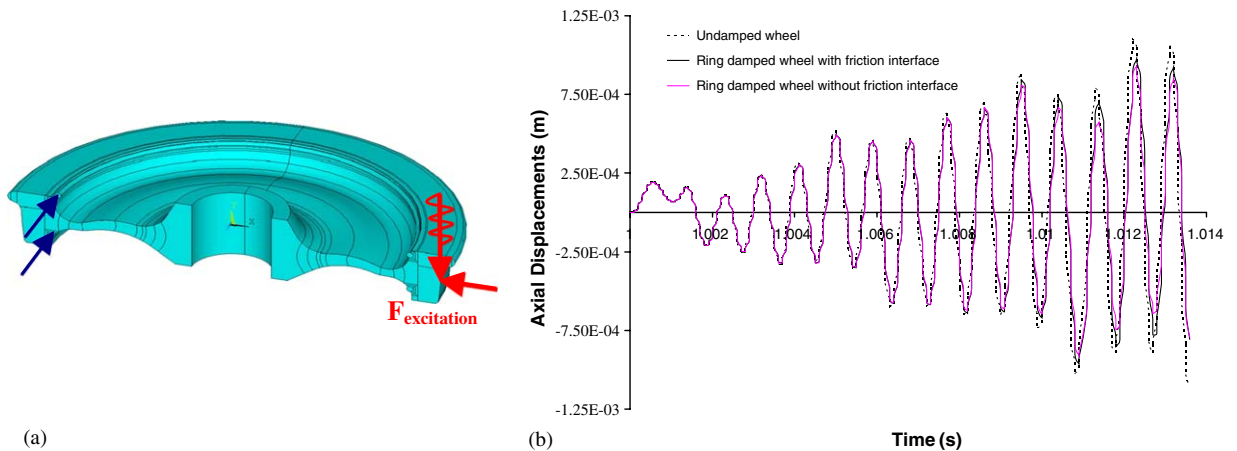


Fig. 8. Three-dimensional model of the ring damped wheel and comparison of the displacements of the undamped and ring damped wheels.

To simulate the preload of the ring into the groove, a pressure on the ring extremities is applied in two steps: a linear increase up to the preload value that is kept constant during the second step.

The steady state is obtained after 14 periods; the time step is 9×10^{-5} s, according to the wheel damping and the contact nonlinearity. Fig. 8b describes the displacements of a point of the web opposed to the excitation point for several computations:

- normal wheel,
- ring damped wheel with friction,
- ring damped wheel without friction.

For the last two periods, a 15% attenuation is obtained between the ring damped wheel and the undamped wheel (Fig. 8b). The ring-groove contact behaviour seems to be the major parameter which acts on the acoustic attenuation. Nevertheless two mechanisms may be distinguished: the friction dissipation or the impact phenomenon. The numerical simulation without friction shows that the impact phenomenon is dominant relative to friction damping and that friction limits the attenuation (19.8% of attenuation without friction). However that accounts for a reduction of 1 dB compared to 10 dB measured in normal use. These results show that the origin of the attenuation is not issued from friction or impact phenomena. Note that these physical mechanisms are generally exposed in the literature as origin of the attenuation. As a perspective another explanation is under investigation by the authors: it is proposed that the attenuation is related to the increase of the rigidity of the system when the ring is preloaded. Coupling of the ring-wheel assembly could modify the dynamic responses of the wheel.

5. Conclusion

A major problem for squeal noise is to identify which mode is prone to squeal within the modal base of the wheel. It has been shown that a harmonic model gives many excited modes with a similar level. A transient analysis has been developed in order to model the lateral creepage variation at the wheel–track contact point. To reduce computation time, an axi-symmetric model of the wheel is used with a harmonic decomposition of displacements and loadings. The transient algorithm is performed in order to update the contact variation with a fine time step. Excitation is modelled as a linear displacement of the hub. The friction law at the wheel–track contact point is a function of the slip velocity. Based on experimental results, a singularity in the friction–velocity relation is modelled. Results show that a reduced number of squealing modes is obtained and that these modes seem to correspond with experiments.

Another interest of transient models is illustrated on the squeal noise attenuation by the ring damping solution. Using the contact model of the ring in the groove, the transient analysis deals with the origin of the attenuation. Even if impact damping is shown to be predominant relative to friction damping, these two mechanisms seem not to be sufficient to explain the observed lower noise levels of ring damping wheels. Two ways of investigations are proposed: a theoretical study of the progressive coupling of the ring–wheel assembly when the ring is preloaded, experimental investigations in a reverberant room with specific set-up in order to highlight the origin of the attenuation.

Acknowledgements

Financial support from the FEDER and the Région Nord Pas de Calais is gratefully acknowledged.

References

- [1] M. Rudd, Wheel/rail noise—part 2: wheel squeal, *Journal of Sound and Vibration* 46 (1976) 381–394.
- [2] D.J. Thompson, C.J.C. Jones, A review of the modelling of wheel–rail noise generation, *Journal of Sound and Vibration* 231 (2000) 519–536.
- [3] K.L. Johnson, *Contact Mechanics*, Cambridge University Press, Cambridge, 1985 pp. 264–269.
- [4] E. Verheijen, R. Van Haaren, J. Van Den Brink, A measurement protocol for curve squeal noise, in: *Proceedings of Internoise*, Nice, 2000, pp. 1573–1579.
- [5] J.-F. Brunel, P. Dufrenoy, J. Charley, F. Demilly, Attenuation of the squeal noise of a railway wheels using metallic rings, in: *Proceedings of the Tenth International Congress of Sound and Vibration*, Stockholm, July 2003, pp. 1681–1690.
- [6] J.F. Brunel, P. Dufrenoy, F. Demilly, Modelling of squeal noise attenuation of ring damped wheels, *Applied Acoustics* 65 (2004) 457–471.
- [7] P.P. Kooijman, W.J. van Vliet, M. Janssens, F. de Beer, Curve squeal of railbound vehicles—part 2: set-up for measurement of creepage dependent friction coefficient, in: *Proceedings of Internoise 2000*, vol. 3, Nice, pp. 1564–1567.
- [8] M. Heckl, A curve squeal of train wheels—part 1, *Journal of Sound and Vibration* 229 (1999) 669–693.
- [9] O. Chiello, Stability analysis, time-domain solutions and vertical dynamics in the modelling of curve squeal generated by rail bound vehicles, in: *Proceedings of the Euronoise*, Naples, 2003, paper ID: 168, pp. 1–6.
- [10] P. Wetta, F. Demilly, Reduction of wheel squeal noise generated on curves or during braking, in: *Proceeding of congrès des essieux montés*, Paris, 1995.
- [11] P. Wetta, F. Sulin, F. Demilly, *Sound measurements on Valdunes ring damped wheels for mass transit railway corporation*, Internal Report, Hong Kong, 1995.
- [12] J. Vinolas, Ring damped wheel solution report, Silent freight, Technical Report, ref: 3F8U12T1, 1998.
- [13] I. Lopez, Theoretical and Experimental Analysis of a Ring-Damped Railway Wheels, Ph.D. Thesis, Universidad de Navarra, 1999.
- [14] J.F. Brunel, P. Dufrenoy, J. Charley, J.L. Munoz, F. Demilly, Optimization of squeal noise attenuation of ring damped wheels, in: *Proceedings of Technological Innovation for Land Transportation*, Lille, December 2003, pp. 611–618.